



# Finite difference modelling of natural convection flow with thermophoresis

S. Jayaraj

*Department of Mechanical Engineering, Regional Engineering College, Calicut, India*

692

Received February 1997  
 Revised November 1997  
 Accepted November 1998

**Keywords** *Finite differences, Natural convection, Thermophoresis*

**Abstract** *Deals with thermophoretic analysis in natural convection laminar flow over a cold vertical flat plate. The governing equations are solved by finite difference marching technique. Variation of wall concentration and wall flux with respect to the plate length is studied. Influence of Prandtl number, plate temperature on particle deposition and wall flux is presented in graphical form. An already established self-adaptive grid generation technique and variable grid size method are incorporated in the computer routine to get more accurate results. The nature of variation of particle concentration profile with respect to Prandtl number is found to be similar. For a cold plate it is observed that the wall concentration increases with decrease in Prandtl number.*

## Nomenclature

Lower case symbols given in parenthesis are the dimensional counterparts of the dimensionless quantities denoted by upper case symbols on the same line.

$C(c)$	= particle concentration	$X, Y(x, y)$	= coordinates along and normal to the plate respectively
$c_p$	= specific heat of the gas-particle mixture at constant pressure		
$k$	= thermal conductivity of gas-particle mixture	<i>Greek symbols</i>	
$K$	= thermophoretic coefficient	$\Delta X, \Delta Y$	= mesh sizes in X, Y directions
$g_x$	= x-component of the acceleration due to gravity	$\nu$	= kinematic viscosity of the gas
$Gr$	= Grashoff number	$\mu$	= absolute viscosity of the gas
$Pr$	= Prandtl number	$\rho$	= density of the gas
$U, V(u, v)$	= velocity components in X, Y(x, y) directions	$\beta$	= compressibility of the gas
$T(t)$	= temperature	<i>Subscripts</i>	
$V_T(v_t)$	= thermophoretic velocity component normal to the plate	$i, j$	= location in X, Y directions respectively
		$w$	= value at the plate surface or wall
		$\infty$	= value in the free stream

## Introduction

Thermophoresis is a phenomenon by which submicron sized particles suspended in a non-isothermal gas acquire a velocity relative to the gas in the direction of decreasing temperature. The velocity acquired by the particles is called thermophoretic velocity and the force experienced by the suspended particles due to the temperature gradient is known as thermophoretic force. The magnitude of thermophoretic force and velocity is proportional to the temperature gradient and depends on many factors like thermal conductivity of

---

aerosol particles and carrier gas, thermophoretic coefficient, heat capacity of the gas and Knudsen number. Thermophoresis causes small particles to deposit on cold surfaces. Repulsion of particles from hot objects will also take place and a particle-free layer is observed around hot bodies. Thermophoresis is considered to be important for particles of  $10\mu\text{m}$  in radius and temperature gradient of the order of  $5\text{K}/\text{mm}$ .

A common example of this phenomenon is blackening of the glass globe of a kerosene lantern. The temperature gradient developed between the flame and the glass globe drives the carbon particles produced in the combustion process towards the globe, where they deposit. There are several other practical situations where we come across this phenomenon, like gas “clean up”, corrosion of heat exchangers with attendant reduction of heat transfer coefficient, fouling of gas turbine equipment, coagulation of condensing/evaporating aerosols, in determining particle trajectories in the exhaust gas from combustion devices, in the transpiration cooling of gas turbine blades, etc. Thermophoresis is considered to be the dominant mass transfer mechanism in the modified chemical vapor deposition (MCVD) process as currently used in the manufacturing of graded index optical fiber preforms. Thermophoretic deposition of radioactive particles is considered to be one of the important factors causing accidents in nuclear reactors.

Thermophoresis in laminar flow over a horizontal flat plate has been theoretically studied by Goren (1977). He analyzed for both cold and hot plate conditions. Homsy *et al.* (1981) has used Blasius series for determining thermophoretic deposition of small particles. Gokoglu and Rosner (1984a) arrived at correlation for deposition rates in forced convection systems with variable properties. The thermophoretic deposition of laminar slot jet on an inclined plate for hot, cold and adiabatic plate conditions were presented earlier by Garg and Jayaraj (1988). Verms (1979) has studied the deposition rates in cooled and uncooled turbine cascades. It was found that temperature difference between the wall and the gas could cause a 15-fold increase in deposition rate as compared with the case of adiabatic cascade. Shen (1989) analyzed the problem of thermophoretic of small particles on to cold surfaces in two-dimensional and axisymmetric cases and this is illustrated with examples of thermophoretic deposition of particles in flow past a cold cylinder and a sphere. Gokoglu and Rosner (1984b) studied the effect of particulate thermophoresis in reducing the fouling rate advantage of effusion cooling in gas turbines. Correlation has been developed to predict thermophoretically enhanced diffusional deposition rates, including the effects of transpiration cooling. We have also studied (Garg and Jayaraj, 1990) the thermophoretic transport of aerosol particles through a forced convection laminar boundary layer in cross flow over a cylinder. In that analysis a finite difference solution was obtained for hot, cold and adiabatic wall conditions.

Wang *et al.* (1985) studied the influence of volumetric heating by axial laser and forced convection motion of aerosol particles in a vertical tube. They found that natural convection is induced by a volumetric heat source associated with

laser absorption. Laser heating of particles or gas accomplishes a significant increase in deposition efficiency. Epstein *et al.* (1985) have carried out thermophoretic analysis of small particles through a free convection boundary layer adjacent to a cold vertical surface. The gas-particle governing equations are solved numerically by defining transformed variables.

The present work is concerned with thermophoresis in two-dimensional natural convection flow over a cold vertical plate. This work was carried out as a prelude of the analysis of soot particle deposition on chimneys. Also, this work will be extended to the case of particle deposition on channel walls. The latter is a convenient preposition for the laser modification of thermophoretic deposition, which finds potential use in the MCVD process. The gas-particle governing equations are made nondimensional and solved by a finite difference marching technique. The effects of Prandtl number and thermophoretic coefficient on particle deposition were studied. Variation of wall concentration with respect to thermophoretic coefficient and the variation of wall flux with respect to plate length are studied for different Prandtl numbers and wall temperatures. Thermophoretic flow analysis with Prandtl number value in the range of liquid metals is presented, which finds application in nuclear engineering. Velocity, temperature and particle concentration profiles are drawn at different longitudinal locations over the wall.

### Governing equations

A warm gas with suspended aerosol particles is considered to be exposed to a cold vertical plate as shown in Figure 1. The temperature gradient developed between the plate and the gas particle mixture drives the particles towards the plate, where they get deposited. The particles are assumed to be sufficiently dilute, so that the physical properties of the mixture are those of the gas only. For particles of unit density and  $1\mu\text{m}$  radius, this assumption limits the analysis to aerosol concentration less than  $10^7$  particles/cm<sup>3</sup> of gas at normal temperature and pressure (Epstein *et al.*, 1985). The velocity and temperature distributions are therefore governed by usual free convection boundary layer equations. For steady, laminar, two-dimensional, incompressible flow with constant properties, the governing equations in nondimensional form are

$$\frac{\partial U}{\partial X} + \frac{\partial V}{\partial Y} = 0, \quad (1)$$

$$U \frac{\partial U}{\partial X} + V \frac{\partial U}{\partial Y} = \frac{\partial^2 U}{\partial Y^2} + T, \quad (2)$$

$$U \frac{\partial T}{\partial X} + V \frac{\partial T}{\partial Y} = \frac{1}{Pr} \frac{\partial^2 T}{\partial Y^2}, \quad (3)$$

$$V_T = \frac{K}{t_\infty / (t_w - t_\infty) + T} \frac{\partial T}{\partial Y}, \quad (4)$$

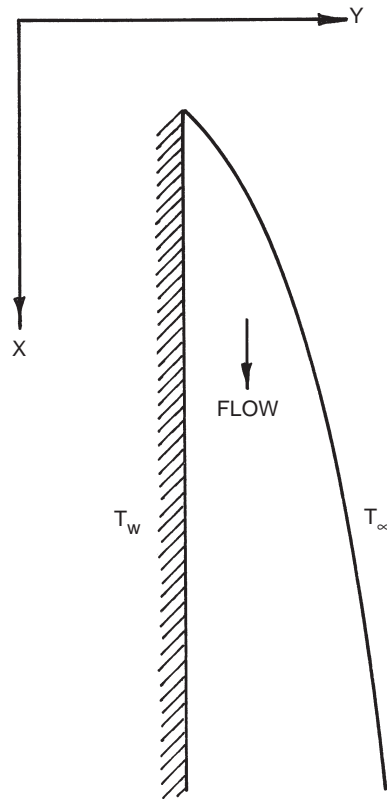


**Figure 1.**  
Physical configuration  
and co-ordinate system

$$U \frac{\partial C}{\partial X} + V \frac{\partial C}{\partial Y} + \frac{\partial(CV_T)}{\partial Y} = 0, \quad (5)$$

where the dimensionless quantities chosen are (Hornbeck, 1973)

$$X = x/L(Gr), Y = y/L, U = uL/\nu(Gr), V = vL/\nu,$$

$$T = (t - t_\infty)/(t_w - t_\infty), V_T = v_t L/\nu, C = c/c_\infty,$$

$$Pr = \mu c_p/k \quad \text{and} \quad Gr = g_x \beta (t_w - t_\infty) L^3 / \nu^3.$$

The boundary conditions are

$$U(X, 0) = 0, U(X, \infty) = 0, U(0, Y) = 0, V(X, 0) = 0,$$

$$T(X, 0) = 1, T(X, \infty) = 0, T(0, Y) = 0,$$

$$C(X, \infty) = 1 \quad \text{and} \quad C(0, Y) = 1. \quad (6)$$

The partial differential governing equations (1)-(3) are coupled and nonlinear in nature. Finite difference method can be applied for solving these equations by using the appropriate discretisation scheme.

**Finite element solution**

To represent the differential equations in finite difference form, a two-dimensional rectangular mesh is superimposed over the flow domain of interest. Indices (i,j) are used to represent the position of a point in the boundary layer. The plate is represented by j = 0 and the outer edge of the boundary layer is represented by j = n+1. The stagnation point corresponds to i = 0.

Equations (2) and (3) are discretised by taking forward difference scheme along the longitudinal X-direction and central difference scheme along the transverse Y-direction. This provides second order accurate solution for U and T. For discretising continuity and thermophoretic velocity equation, forward difference scheme is used. The finite difference forms chosen for the particle conservation equation are of first order accurate for C. The discretised forms of the governing equations (1)-(5) are given below:

$$\frac{U_{i+1,j+1} - U_{i,j+1}}{\Delta X} + \frac{V_{i+1,j+1} - V_{i+1,j}}{\Delta Y} = 0 \tag{7}$$

$$U_{i+1,j} \frac{U_{i+1,j} - U_{i,j}}{\Delta X} + V_{i+1,j} \frac{U_{i+1,j+1} - U_{i+1,j-1}}{2(\Delta Y)} = \frac{U_{i+1,j+1} - 2U_{i+1,j} + U_{i+1,j-1}}{\Delta Y^2} + T_{i+1,j} \tag{8}$$

$$U_{i+1,j} \frac{T_{i+1,j} - T_{i,j}}{\Delta X} + V_{i+1,j} \frac{T_{i+1,j+1} - T_{i+1,j-1}}{2(\Delta Y)} = \frac{1}{Pr} \frac{T_{i+1,j+1} - 2T_{i+1,j} + T_{i+1,j-1}}{\Delta Y^2} \tag{9}$$

$$V_{T_{i+1,j}} = \frac{-K}{[1/(t_w/t_\infty) - 1] + T_{i+1,j}} \frac{T_{i+1,j+1} - T_{i+1,j}}{\Delta Y} \tag{10}$$

$$U_{i+1,j} \frac{C_{i+1,j} - C_{i,j}}{\Delta X} + V_{i+1,j} \frac{C_{i+1,j+1} - C_{i+1,j}}{\Delta Y} + \frac{C_{i+1,j+1} V_{T_{i+1,j+1}} - C_{i+1,j} V_{T_{i+1,j}}}{\Delta Y} = 0 \tag{11}$$

$$U_{i+1,j} \frac{C_{i+1,j} - C_{i,j}}{\Delta X} + V_{i+1,j} \frac{C_{i+1,j} - C_{i+1,j-1}}{\Delta Y} + \frac{C_{i+1,j+1} V_{T_{i+1,j+1}} - C_{i+1,j} V_{T_{i+1,j}}}{\Delta Y} = 0 \tag{12}$$

The truncation error is of O(ΔX) and O(ΔY<sup>2</sup>) for momentum and energy equations and O(ΔX) and O(ΔY) for continuity and particle conservation

---

equations. The two different types of discretisation of concentration equation, (11) and (12), are required mainly to satisfy the conditions of Thomas algorithm, which is used to obtain the solutions.

The velocities and temperatures are to be calculated simultaneously due to the coupling between momentum and energy equations. Also equations (8) and (9) are not linear. Hence an iterative procedure is required to obtain a solution. A marching procedure starting from the location  $X = 0$  is followed to determine the solution for  $U$ ,  $V$ ,  $T$  and  $C$ . The discretised momentum equation written for  $j = 1(n)$  constitutes  $n$  linear equations and are solved by tridiagonal algorithm.  $V$  values are computed by using the recently obtained  $U$  values. To solve the energy equations the new values of  $U$  and  $V$  are used. Thus the iterative procedure consists of solving the set of discretised momentum, continuity and energy equations in that order repeatedly until converged solution is obtained for  $U$ ,  $V$  and  $T$ . These values are used to get  $V_T$  and  $C$  using equations (10) and (11) or (12).  $U$ ,  $V$ ,  $T$  and  $C$  values obtained at one  $X$ -location are used to get the corresponding values in the next  $X$ -location. Marching is continued until the boundary layer development is almost complete.

### Computational details

A computational scheme followed for an earlier work (Garg and Jayaraj, 1988) is used for the present analysis also. This scheme takes care of boundary layer adjustment as marching proceeds away from the leading edge. Velocity, temperature and concentration boundary layers are adjusted separately. Grid size is changed along the  $X$ -direction with initial  $\Delta X$  as 0.0001.  $\Delta X$  is doubled after 20 steps initially. The self-adaptive grid generation method suggested by Nakahashi and Deiwert (1987) is incorporated in the computer routine. This method automatically selects fine mesh size in the regions of larger concentration gradient and coarse mesh size in the other regions. The minimum and maximum  $\Delta Y$  values are selected as 0.025 and 0.25 respectively, for the results presented in this paper. These values are selected after the verification of mesh convergence and validation of the results as explained in the next section. When the minimum and maximum  $\Delta Y$  values are doubled or halved the change in the results obtained was found to be only on the third decimal place. It is determined through numerical experimentation that calling the adaptation subroutine after every 25 steps of marching is most efficient. However, for the first 25 steps  $\Delta Y$  is kept constant as 0.05.

### Results and discussion

Ostrach (cf. Hornbeck, 1973) has calculated the velocity and temperature boundary layers over the vertical flat plate using the finite difference method. Hence the results of longitudinal velocity and temperature boundary layers by finite difference method obtained using the present computer code is not new. The velocity and temperature profiles obtained were compared with the solution presented by Ostrach to check the correctness of the solution procedure and the computer code used. Very close agreement of the

hydrodynamic and thermal boundary layer results were noticed. Thermophoresis in natural convection flow over a flat plate considering the working fluid as air ( $Pr = 0.73$ ) was studied by Epstein *et al.* (1985). The governing equations were solved by them using similarity solution. As elaborated before, the results are obtained in the present study by a finite difference marching procedure. The particle concentration profiles are drawn at several X-locations and for different Prandtl numbers. The variation of wall flux along the plate, the effect of Prandtl numbers and plate temperature on wall flux are studied. The effect of Prandtl number, thermophoretic coefficient and plate temperature on particle deposition is also presented.

*Concentration profiles*

Figures 2-4 show the particle concentration profiles drawn at six X-locations ( $X = 0.05, 0.1, 0.3, 0.5, 0.7$  and  $1.0$ ) and for three Prandtl number values ( $Pr = 1.5, 1.0$  and  $0.05$ ). In the case of cold wall conditions a non-zero particle concentration at the wall is expected. Hence, the concentration profiles start from positive values at the wall and gradually increase and reach the free stream value. The nature of variation of concentration profiles for gases and liquid metals is found to be same. However, for liquid metals the wall concentration due to thermophoresis is more compared to that for gases due to

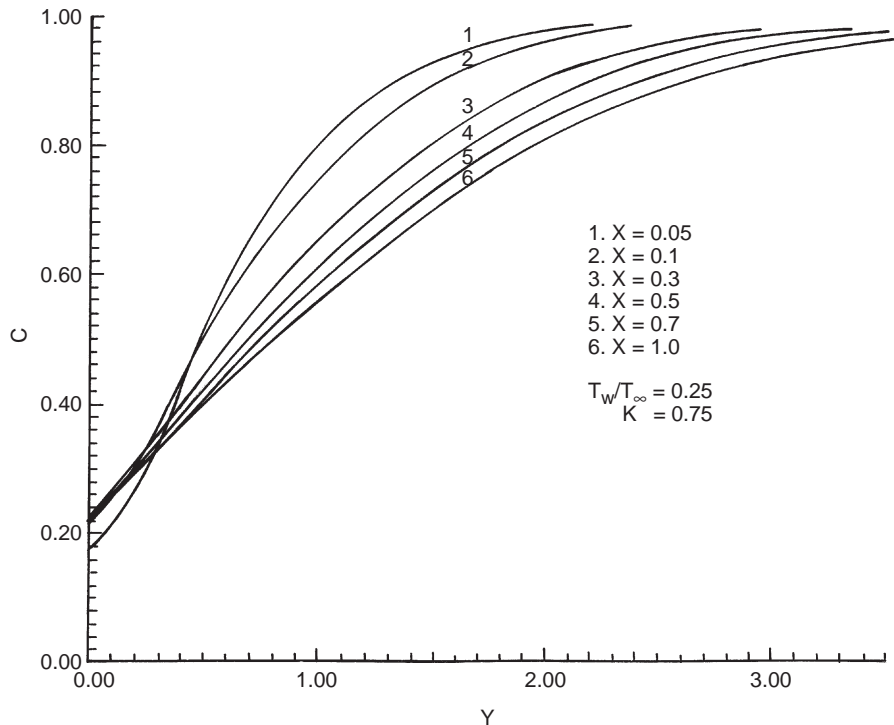


**Figure 2.**  
Particle concentration profiles ( $Pr = 1.5$ )

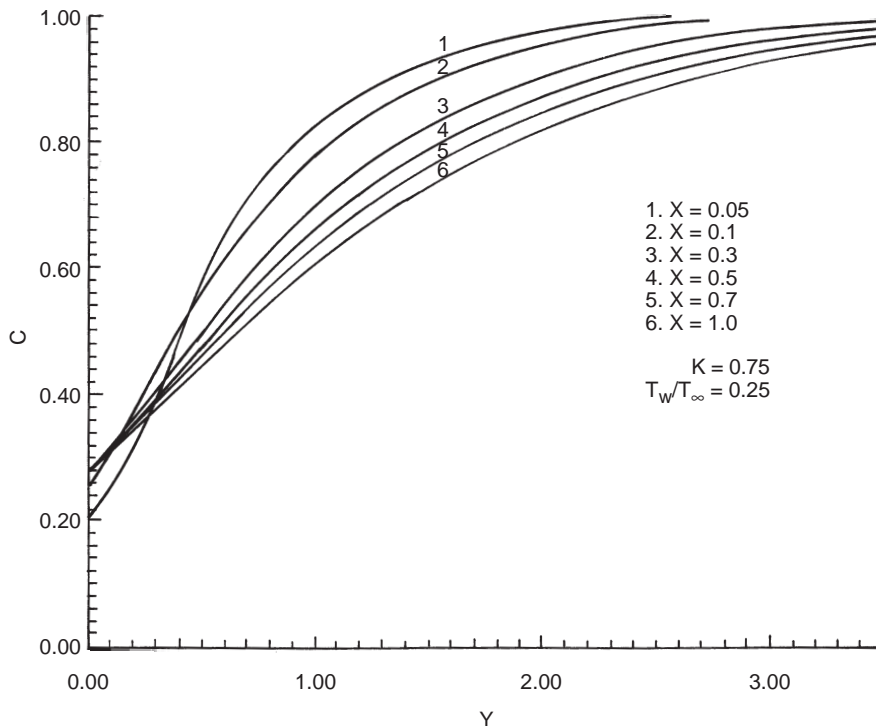


**Figure 3.**  
Particle concentration  
profiles ( $Pr = 1.0$ )

the fact that thermal diffusivity is more for liquid metals. So, the particle movement will be in such a way that more and more particles get collected near the wall. Particle concentration profiles are also drawn with  $Pr = 0.73$  and  $K = 0.5$ , for comparing with the results of Epstein *et al.* (1985). The obtained result by the present method and that of Epstein *et al.* (1985) are shown in Figure 5. It can be seen in this figure that the concentration profiles obtained are in good agreement with that of the literature value.

#### Wall concentration curves

Variation of wall concentration with respect to  $X$  is shown in Figure 6. It is found that  $C_w$  is zero at the leading edge.  $C_w$  increases up to certain  $X$  and then remains constant. It is found that irrespective of the Prandtl number value, nature of variation of  $C_w$  remains the same. However, the magnitude of wall concentration increases with a decrease in Prandtl number. With an increase in Prandtl number thermal diffusivity decreases and hence the particle collection on cold surface decreases.

The effect of thermophoretic coefficient (which is treated as constant and independent of temperature in the present analysis) on wall concentration is also studied. Wall concentration curves are drawn with respect to thermophoretic coefficient for two different wall temperature ratios of 0.25 and 0.50. These curves are shown in Figure 7. It is found that as  $K$  increases  $C_w$



HF  
9,6

700

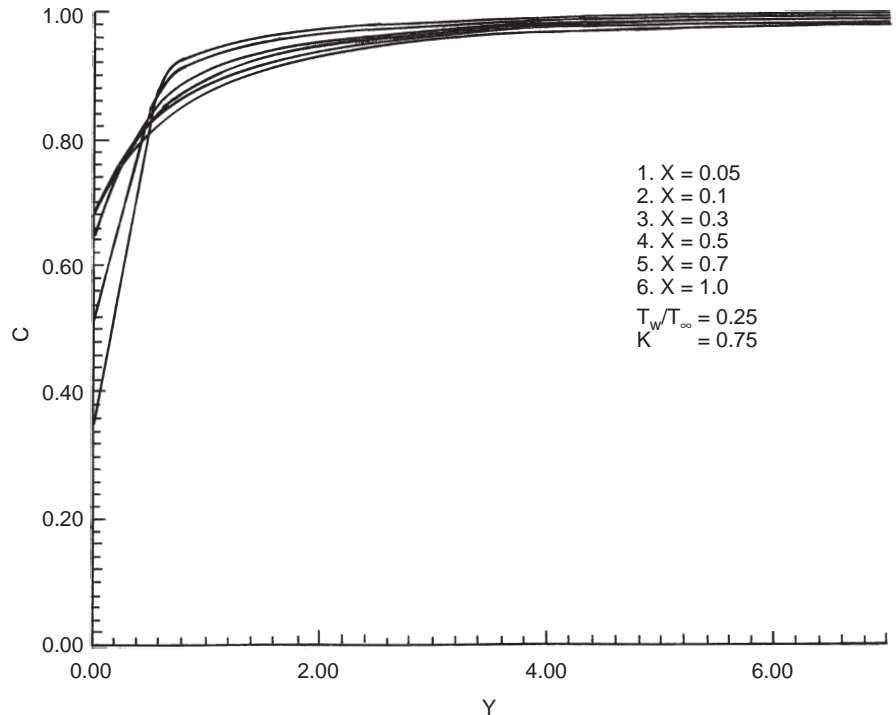


**Figure 4.**  
Particle concentration  
profiles ( $Pr = 0.05$ )

decreases. When  $K = 0$ , there is no thermophoresis and aerosol particles move with the same velocity as the gas (the thermophoretic velocity being zero in this case). The thermophoretic coefficient depends on Knudsen number value. Large value of  $K$  means the Knudsen number is large, corresponding to which the thermophoretic force is small. Hence, wall concentrations are less at larger values of  $K$ . It is also observed that with increase in temperature ratio, wall concentration increases.

#### *Wall flux curves*

The local dimensionless concentration flux at the wall  $-(V_T C)_w$  as defined by Homsy *et al.* (1981) are drawn with respect to the plate length, for two different Prandtl numbers ( $Pr = 0.73$  and  $0.05$ ) and for two wall temperature ratios of  $0.25$  and  $0.50$  (Figures 8 and 9). It is found that variation of wall flux is identical for both the temperature ratios. The wall flux increases up to a certain  $X$  and reaches maximum around  $X \cong 0.2$  and thereafter decreases to attain a constant value asymptotically. It is also observed that wall flux increases with decrease in the temperature ratio. This is due to the fact that, as the temperature ratio increases wall concentration is more and thermophoretic velocity is less. Hence the product  $-(V_T C)_w$  becomes less than that for the lower temperature ratio values. From the wall flux curves shown in Figures 8 and 9 it is clear that, for gases with increased Prandtl number, the maximum wall flux decreases.

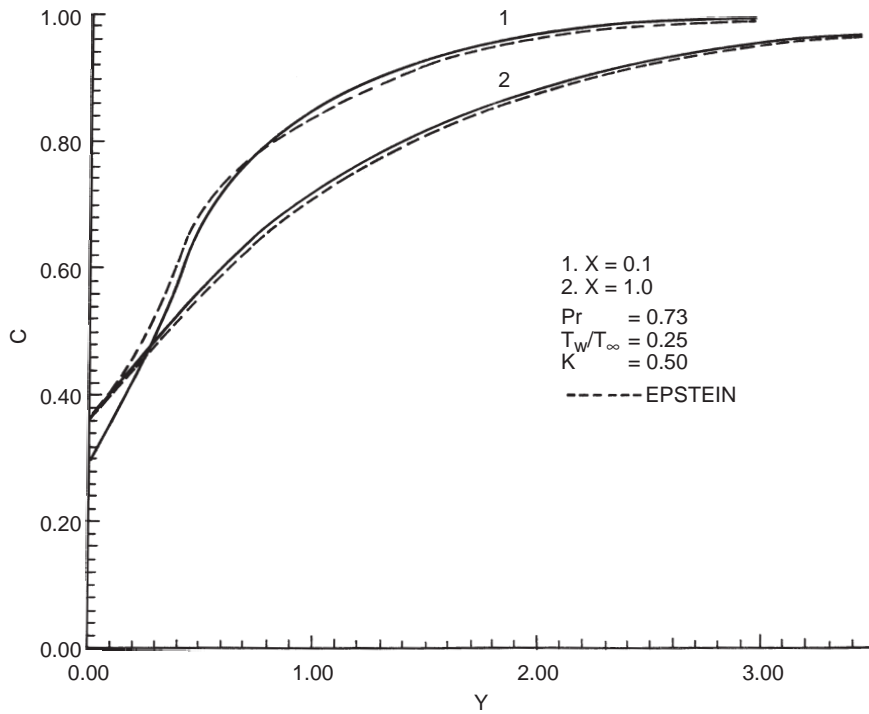


**Figure 5.**  
Particle concentration  
profiles ( $Pr = 0.73$ )

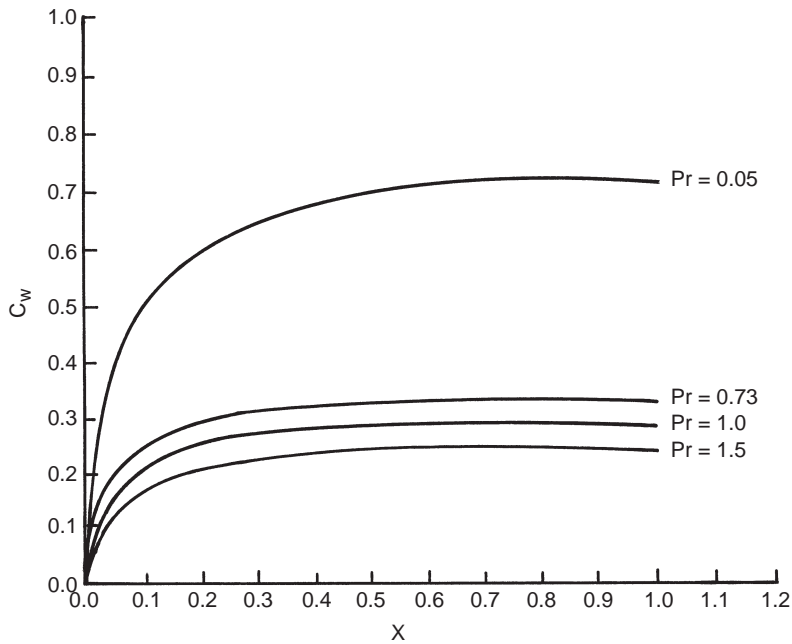


**Figure 6.**  
Wall concentration  
along the plate length

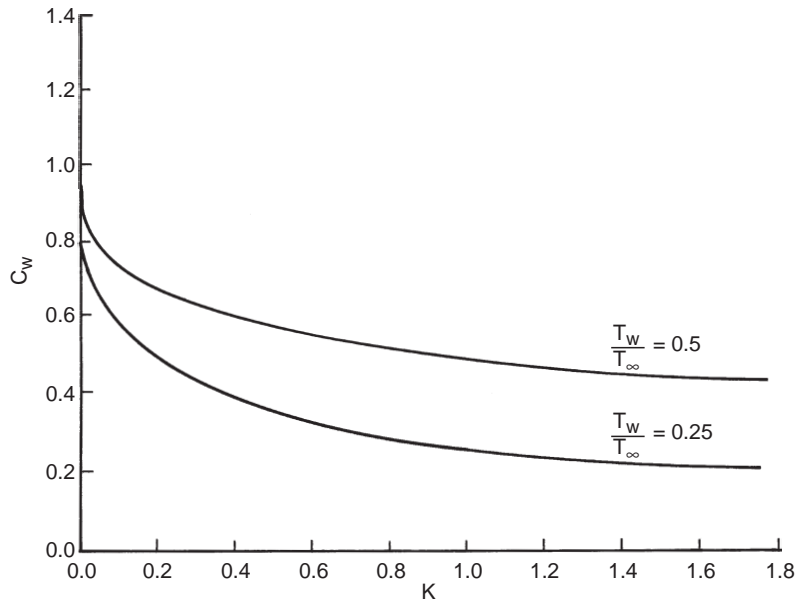


**Figure 7.**  
Wall concentration with respect to thermophoretic coefficient

### Conclusions

Thermophoretic particle concentration calculations for the natural convection boundary layer on a cold vertical flat plate for laminar flow are carried out. The

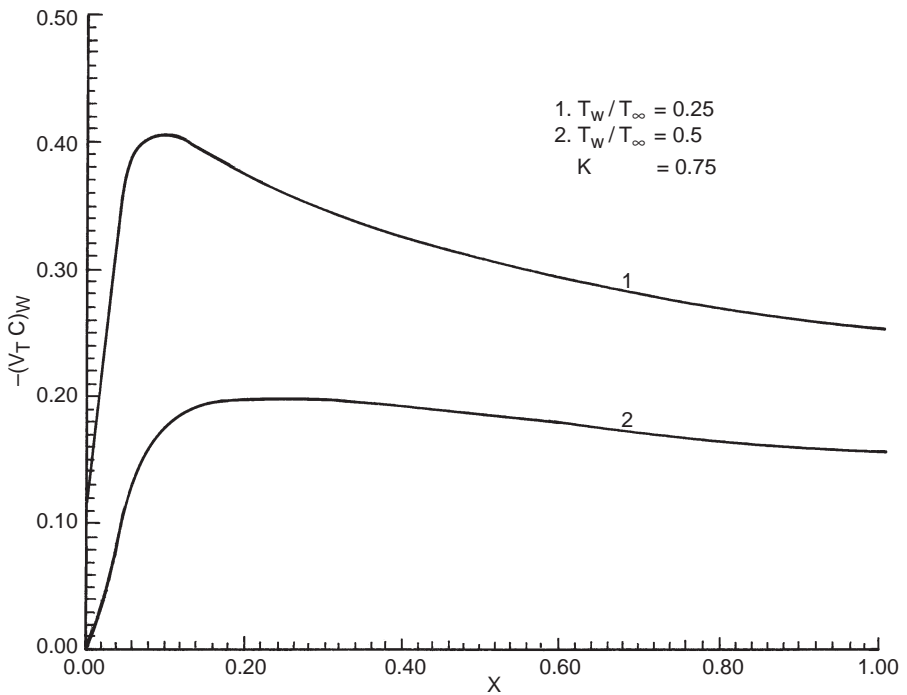


**Figure 8.**  
Wall flux curves ( $Pr = 0.73$ )

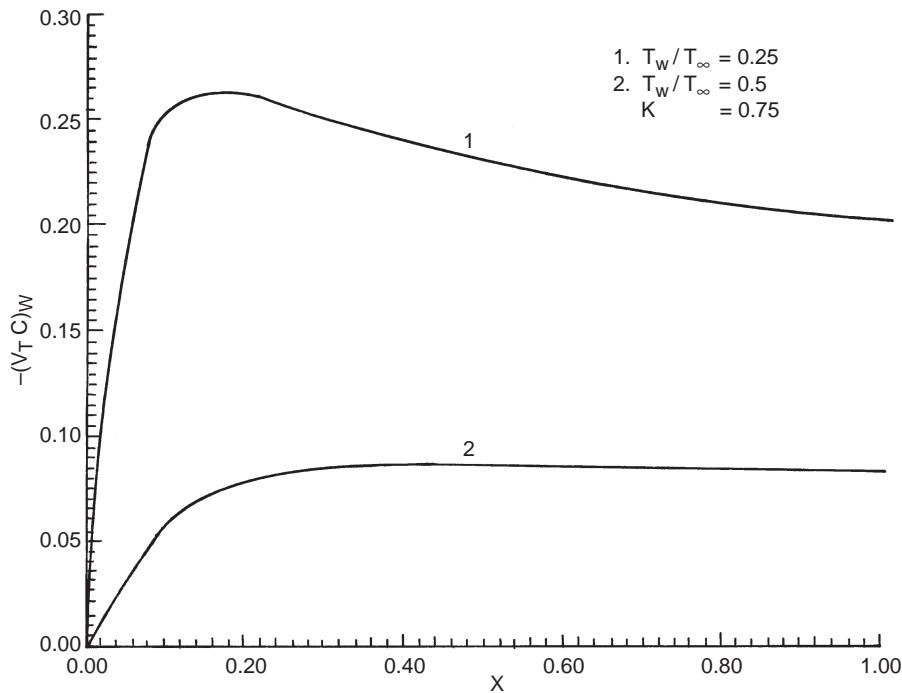


**Figure 9.**  
Wall flux curves ( $Pr = 0.05$ )

governing equations are solved by finite difference marching procedure. Graphs are plotted for velocity, temperature and particle concentration in the boundary layer. From the analysis it is observed that wall concentration increases with decrease in Prandtl number. Except the region very close to the leading edge, wall concentration remains constant. Thermophoretic coefficient affects wall concentration and with increase in thermophoretic coefficient wall concentration decreases. With increase in plate temperature wall concentration increases. It is found that for gases ( $Pr \cong 0.73$ ) wall flux decreases with increase in Prandtl number. For liquid metals ( $Pr \cong 0.05$ ) deposition due to thermophoresis is more than that of gases. The effect of Prandtl number and wall temperature on wall concentration and wall flux are also presented. Further analysis on thermophoretic deposition with variable properties, laser modification and channel flow is underway. The results presented here are of much value for comparison and better understanding of the thermophoresis phenomenon.

#### References

- Epstein, M., Houser, G.M. and Henry, R.E. (1985), "Thermophoretic deposition of particles in natural convection flow from a vertical plate", *J. Heat Transfer*, Vol. 107, pp. 272-6.
- Garg, V.K. and Jayaraj, S. (1988), "Thermophoresis of aerosol particles in laminar flow over inclined plates", *Int. J. Heat Mass Transfer*, Vol. 31, pp. 875-90.

- 
- Garg, V.K., and Jayaraj, S. (1990), "Thermophoretic deposition over a cylinder", *Int. J. Eng. Fluid Mech.*, Vol. 3, pp. 175-96.
- Gokoglu, S.A. and Rosner, D.E. (1984a), "Correlation of thermophoretically-modified small particle diffusional deposition rates in forced convection systems with variable properties, transpiration cooling and/or viscous dissipation", *Int. J. Heat Mass Transfer*, Vol. 27, pp. 639-46.
- Gokoglu, S.A. and Rosner, D.E. (1984b), "Effect of particulate thermophoresis in reducing the fouling rate advantages of effusion-cooling", *Int. J. Heat Fluid Flow*, Vol. 5, pp. 37-41.
- Goren, S.L. (1977), "Thermophoresis of aerosol particles in the laminar boundary layer on a flat plate", *J. Colloid Interface Sci.*, Vol. 61, pp. 77-85.
- Homsy, G.M., Geyling, F.T. and Walker, K.L. (1981), "Blasius series for thermophoretic deposition of small particles", *J. Colloid Interface Sci.*, Vol. 83, pp. 495-501.
- Hornbeck, R.W. (1973), *Numerical Marching Techniques in Fluid Flows with Heat Transfer*, NASA SP-297, Washington, DC.
- Nakahashi, K. and Diewert, G.S. (1987), "Self-adaptive grid method with application to airfoil flow", *AIAA J.*, Vol. 25, pp. 513-20.
- Shen, C. (1989), "Thermophoretic deposition of particles on to cold surfaces in two-dimensional and axi-symmetric flows", *J. Colloid Interface Sci.*, Vol. 127, pp. 104-15.
- Vermes, G. (1979), "Thermophoresis-enhanced deposition rates in combustion turbine blade passages", *J. Eng. Power*, Vol. 101, pp. 542-8.
- Wang, C.Y., Morse, T.F. and Cipolla, J.W. (1985), "Laser-induced natural convection and thermophoresis", *J. Heat Transfer*, Vol. 107, pp. 161-7.